

# Size Dependence and Convergence of the Retrieval Parameters of Metamaterials

Jiangfeng Zhou,<sup>1,2</sup> Thomas Koschny,<sup>1,3</sup> Maria Kafesaki,<sup>3</sup> and Costas M. Soukoulis<sup>1,3</sup>

<sup>1</sup>*Ames Laboratory and Department of Physics and Astronomy, Iowa State University, Ames, Iowa 50011*

<sup>2</sup>*Department of Electrical and Computer Engineering and Microelectronics  
Research Center, Iowa State University, Ames, Iowa 50011*

<sup>3</sup>*Institute of Electronic Structure and Laser - Foundation for Research and Technology Hellas (FORTH),  
and Department of Materials Science and Technology, University of Crete, Greece*

We study the dependence of the retrieval parameters, such as the electric permittivity,  $\epsilon$ , the magnetic permeability,  $\mu$ , and the index of refraction,  $n$ , on the size of the unit cell of a periodic metamaterial. The convergence of the retrieved parameters on the number of the unit cells is also examined. We have concentrated our studies on the so-called fishnet structure, which is the most promising design to obtain negative  $n$  at optical wavelengths. We find that as the size of the unit cell decreases, the magnitude of the retrieved effective parameters increases. The convergence of the effective parameters of the fishnet as the number of the unit cells increases is demonstrated but found to be slower than for regular split ring resonators and wires structures. This is due to a much stronger coupling between the different unit cells in the fishnet structure.

PACS numbers: 42.70.Qs, 41.20.Jb, 42.25.Bs, 73.20.Mf

## INTRODUCTION

The recent development of metamaterials with negative refractive index has confirmed that structures can be fabricated that can be interpreted as having both a negative effective permittivity,  $\epsilon$ , and a negative effective permeability,  $\mu$ , simultaneously. Since the original microwave experiments for the demonstration of negative index behavior in the split ring resonators (SRRs) and wires structures, new designs have been introduced, such as the fishnet, that have pushed the existence of the negative refractive index at optical wavelengths [1, 2, 3]. Most of the experiments [4, 5, 6, 7, 8] with the fishnet structure measure the transmission,  $T$ , and the reflection,  $R$ , and use the retrieval procedure [9, 10, 11, 12, 13] to numerically obtain the effective parameters,  $\epsilon$ ,  $\mu$  and  $n$ . The only direct experimental way that was able to measure both the phase and the group velocity, was done by pulse measurements [6]. In all the other experiments only  $T$  and/or  $R$  are measured and then the retrieval procedure is used to obtain the effective parameters. There is an unresolved issue in the retrieval procedure, what is the size of the unit cell that needs to be used. Most of the retrieval procedures use only one unit cell and made the assumption that if more than one unit cell will be used, the results will be the same as for the single unit cell. This is an untested assumption and Koschny et al. [11] have systematically studied this assumption for the SRRs and wires. It was found that this assumption is correct if the wavelength is 30 times larger than the size of the unit cell. No systematic study have been done on the dependence of the retrieval parameters on the size of the unit cell of the fishnet structure. In this work, we tackle this problem and also study the convergence of the effective parameters from the retrieval procedure as the number of the unit cells increases. We also, exam-

ine how the figure of merit (FOM), which is defined as  $-\text{Re}(n)/\text{Im}(n)$ , changes with the size of the unit cell and the number of the unit cells.

## NUMERICAL CALCULATIONS

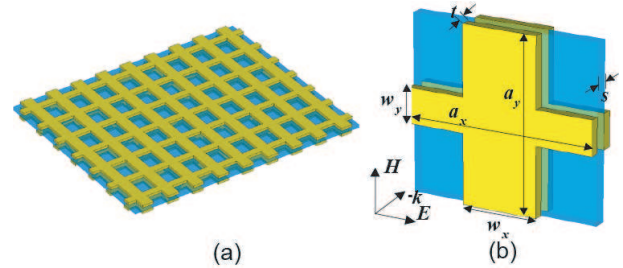


FIG. 1: Schematic of a fishnet structure (a); a single unit cell with geometric parameters marked on it (b).

Our numerical simulations were done with CST Microwave Studio (Computer Simulation Technology GmbH, Darmstadt, Germany), which uses a finite-integration technique, and Comsol Multiphysics, which uses a frequency domain finite element method. The schematics of the unit cell of fishnet structure are shown in Fig. 1(b). Notice that the propagation direction is perpendicular to the plane of the fishnet. In Fig. 2 we present the results for the transmission,  $T$ , reflection,  $R$ , and absorption,  $A = 1 - T - R$ , for a given size of the unit cell.

In Fig. 3, we present the results of the real part of the retrieved effective parameters,  $n$ ,  $\mu$  and  $\epsilon$ , as a function of the frequency. Notice that as the size of the unit cell is getting larger the strength of the resonance of the magnetic permeability  $\mu$  is getting weaker. The same is true

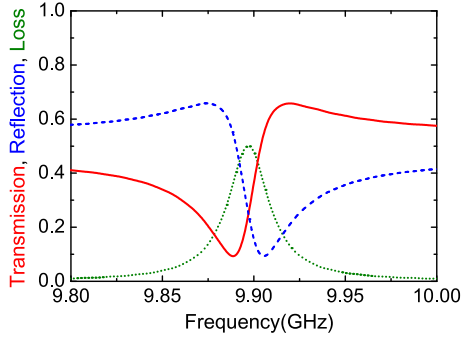


FIG. 2: Simulated transmission (red solid), reflection (blue dashed) and loss (green dotted), which is proportional to absorption, of a fishnet structure. The geometric parameters are  $a_x = a_y = 15$  mm,  $a_z = 4$  mm,  $w_x = 6$  mm,  $w_y = 4$  mm,  $s = 0.5$  mm and  $t = 0.05$  mm and the dielectric constant of the spacer is  $\epsilon = 5$ .

for the magnitude of the index of refraction,  $n$ , which is also negative. For the dimensions we have chosen, the resonance frequency is 9.9 GHz, which is equivalent to a wavelength of  $\lambda = 30.3$  mm. So the ratio of  $\lambda/a_z \approx 30, 15, 7.6$  for the three sizes ( $a_z = 1$  mm, 2 mm and 4 mm) of the unit cell examined in Fig. 3. The real part of  $\epsilon$  is always negative, and shows an anti-resonance [10] corresponding to the magnetic resonance at 9.9 GHz.

Another important issue [14] that the community of metamaterials has not completely understood is why the width of the negative  $n$  is wider than the width of the negative  $\mu$ , as can be seen in Fig. 3(a) and 3(b). In Fig. 4, we plot together the  $\mu$  and  $n$  (real parts) around the magnetic resonance frequency of 9.9 GHz for the  $a_z = 1$  mm case. Notice that  $\mu < 0$  for frequencies higher than 9.9 GHz. However  $n$  is also negative below 9.9 GHz where  $\mu > 0$ . So we have two regions that give negative  $n$ . The one above 9.9 GHz (drawn as blue in Fig. 4) which has both  $\epsilon$  and  $\mu$  negative and therefore  $n$  is also negative. The other region, below 9.9 GHz (shown as yellow in Fig. 4) has  $\epsilon < 0$  but  $\mu > 0$  and still give  $n < 0$ . The reason is that one can obtain  $\text{Re}(n)$  negative provided that  $\text{Im}(\epsilon)\text{Im}(z) > \text{Re}(\epsilon)\text{Re}(z)$ , where  $z = \sqrt{\mu/\epsilon}$ . For the details of this explanation see Ref. [15, 16, 17]. The normalized loss,  $(1 - T - R)/(1 - R)$ , which is the ratio between the absolute loss,  $1 - T - R$ , and the total energy entering the fishnet structure,  $1 - R$ , is also shown in Fig. 4. The normalized loss is a better measure of the absorption in a medium, since it removes the effect of the reflection due to the impedance mismatch at the interface between the medium and the vacuum space, which results in lower absolute loss. If we compare the frequencies with same  $\text{Re}(n)$  value in the regions below 9.9 GHz (yellow) and above 9.9 GHz (blue), one can see that the normalized loss in the region below 9.9 GHz (yellow) is much higher than the region above 9.9 GHz (blue). The transmission,  $T$ , as shown in Fig. 2, in region

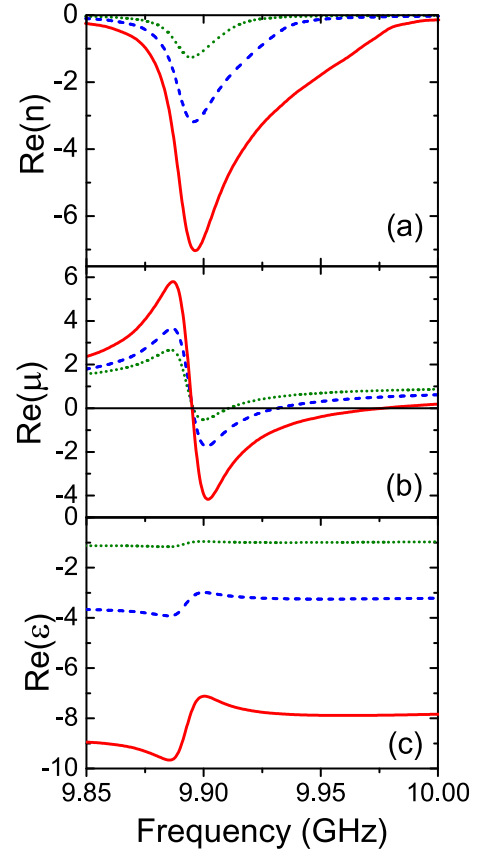


FIG. 3: Retrieved real part of refractive index,  $n$ , (a), permeability,  $\mu$ , (b), and permittivity,  $\epsilon$ , (c), from simulated data shown in Fig. 2, using unit cell size in propagation direction  $a_z = 1$  mm (red solid),  $a_z = 2$  mm (blue dashed) and  $a_z = 4$  mm (green dotted).

above 9.9 GHz (blue) is much higher than in the region below 9.9 GHz (yellow). Therefore, the frequency region above 9.9 GHz (blue) is the frequencies range which is suitable for the applications of the negative refractive index medium.

In Fig. 5, we present the results of the figure of merit ( $\text{FOM} = -\text{Re}(n)/\text{Im}(n)$ ) as the size of the unit cell of the fishnet structure increases. Notice that as the size of the unit cell is getting smaller, the FOM increases and reaches a value of 6.5, when the size of the unit cell along the propagation direction is equal to 1 mm. Notice also that the maximum of the figure of the merit is higher than the resonance frequency, which is 9.9 GHz. The reason is that the  $\text{Im}(n)$  takes its larger value at the resonance frequency and decreases as one goes away from the resonance frequency. This is the reason that the  $\text{FOM} = 6.5$  for  $a_z = 1$  mm has its maximum value at 9.95 GHz.

In Fig. 6, we present the results of the retrieved  $n$ ,  $\mu$  and  $\epsilon$  (real parts only), as a function of frequency, for THz frequencies. As we have discussed above, the fishnet structure is the only structure that has been proven to give negative  $n$  at THz and optical frequen-

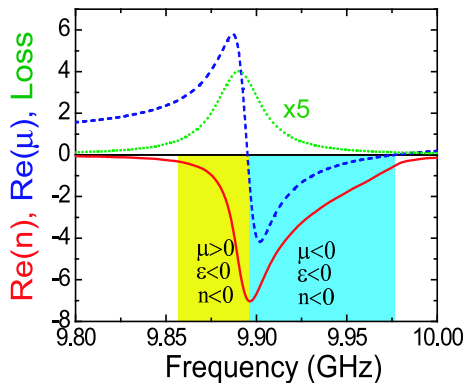


FIG. 4: Retrieved real part of effective refractive index,  $\text{Re}(n)$ , (red solid), permeability,  $\text{Re}(\mu)$ , (blue dashed), and normalized loss,  $(1 - T - R)/(1 - R)$ , (green dotted) (normalized loss has been magnified by a factor of 5 to improve visibility). The shadow regions, below 9.9 GHz (yellow) and above 9.9 GHz (blue), show frequency regions with  $\text{Re}(n) < -0.5$ .

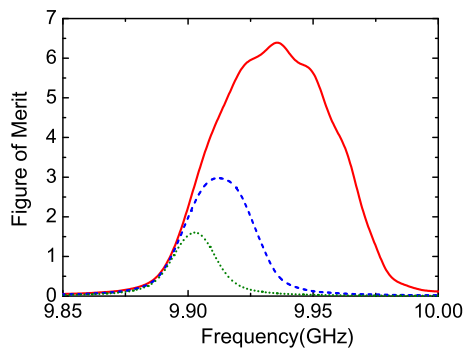


FIG. 5: Figure of merit,  $\text{FOM} = -\text{Re}(n)/\text{Im}(n)$ , for unit cell size  $a_z = 1$  mm (red solid),  $a_z = 2$  mm (blue dashed) and  $a_z = 4$  mm (green dotted).

cies [2, 3, 7, 18]. To obtain negative  $\mu$  and negative  $n$  at THz frequencies, we have to scale down the dimensions given in Fig. 2. The size of the unit cell along the propagation direction  $a_z = 200$  nm, 300 nm and 400 nm. The resonance frequency is approximately 235 THz, which is equivalent to a wavelength  $\lambda = 1.28 \mu\text{m}$ . So the ratio of  $\lambda/a_z = 6.4, 4.27$  and  $3.2$  for the three sizes  $a_z = 200$  nm, 300 nm, and 400 nm of the unit cell examined in Fig. 6. Notice in Fig. 6(a) that as the size of the unit cell increases the retrieved  $n$  goes from negative to positive values. The reason for the positive value of  $n$  is the following: As the size of the unit cell along the propagation direction increases, the effective plasma frequency of the fishnet structure, as shown in Fig. 6(c), decreases and becomes smaller than the magnetic resonance frequency of  $\mu$ , as shown in Fig. 6(b). Therefore, we don't have an overlap of the negative region of  $\epsilon$  and  $\mu$ .

In Fig. 7, we present the results of the transmission of the one unit cell, four unit cells, eight unit cells and ten unit cells (along propagation direction) for a fishnet

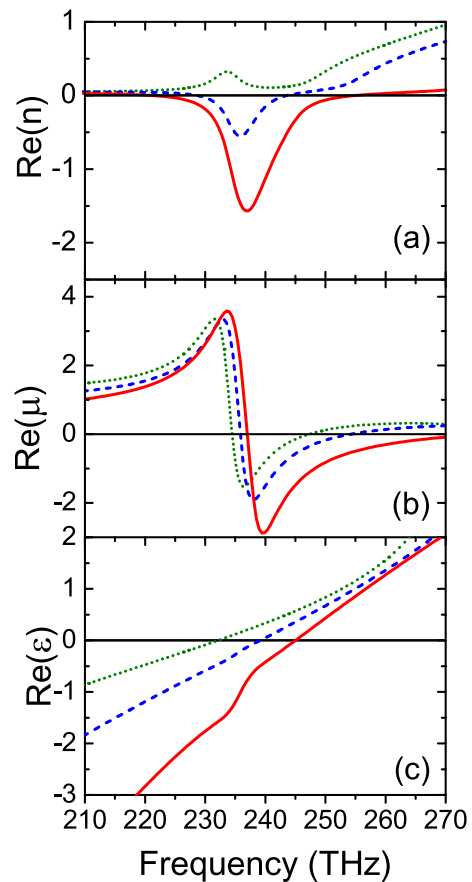


FIG. 6: Retrieved real part of effective refractive index,  $n$ , (a), permeability,  $\mu$ , (b) and permittivity,  $\epsilon$ , (c) from simulation data of a fishnet structure with parameters  $a_z = 200$  nm (red solid),  $a_z = 300$  nm (blue dashed), and  $a_z = 400$  nm (green dotted). The other geometry parameters are  $a_x = a_y = 600$  nm,  $w_x = 400$  nm,  $w_y = 200$  nm,  $s = 100$  nm and  $t = 60$  nm, and the dielectric constant of the spacer is  $\epsilon = 1.9$ .

structure that has a magnetic resonance at 15.65 GHz. Notice that as the number of the unit cells increases, the transmission results converge to a common value. This is seen more clearly in Fig 8, where we present the retrieved results for the effective index of refraction. One can clearly see that the results for eight and ten unit cells are exactly the same. This convergent length dependence is a required property to attribute effective medium behavior to a metamaterial [11]. Notice that the converged results for the effective parameters are different from the effective parameters results of the one unit cell. As one can see from Fig. 8(a), the retrieved results for the effective parameter  $n$  for more than one unit cells are completely different for the results of the one unit cell. This is true, especially when the  $\text{Re}(n)$  is relative large. At the high frequency edges of the negative  $n$  region, there is no much difference between the results of the one unit cell with the results of more than one unit cells. In Fig. 8(b), one notices that the FOM does not change dra-

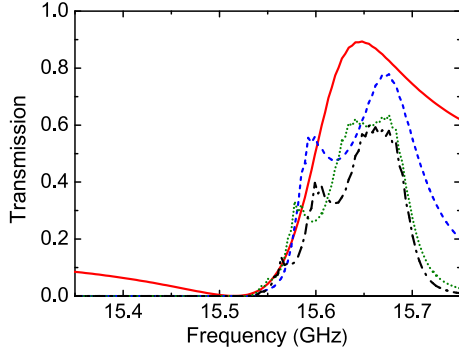


FIG. 7: Simulated transmission spectra of one layer (red solid), four layers (blue dashed), eight layers (green dotted) and ten layers (black dash-dotted) of the fishnet structure. The geometric parameters are  $a_x = a_y = 10$  mm,  $a_z = 4$  mm,  $w_x = 4$  mm,  $w_y = 3$  mm,  $s = 1$  mm and  $t = 0.05$  mm, and the dielectric constant of the spacer is  $\epsilon = 4$ .

matically as one uses more unit cells to do the retrieval procedure. As one uses more unit cells, the FOM has more oscillations as a function of frequency.

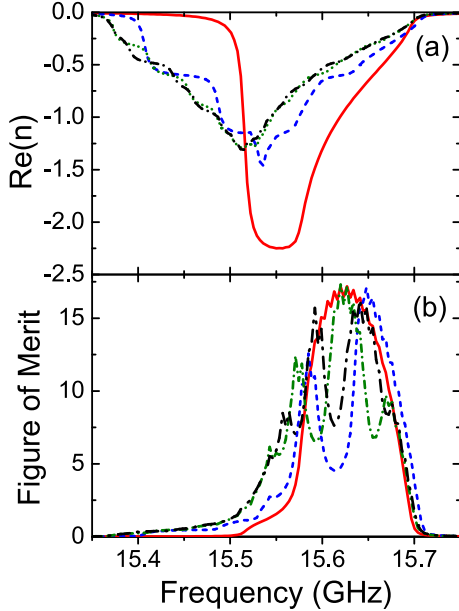


FIG. 8: Retrieved real part of effective refractive index,  $n$ , and figure of merit of the simulated structure described in Fig. 7.

Fig. 9 shows the real parts of effective refractive index,  $\text{Re}(n)$ , as a function of frequency for one layer and two layers fishnet structure with different unit cell size:  $a_z = 1$  mm,  $a_z = 2$  mm and  $a_z = 4$  mm. The resonance frequencies, i.e. frequency with maximum  $|\text{Re}(n)|$ , are 9.926 GHz (red dashed), 9.896 GHz (blue dashed) and 9.894 GHz (green dashed) for one layer; 9.973 GHz (red solid), 9.927 GHz (blue solid) and 9.900 GHz (green solid) for two layers. The difference in value of resonance

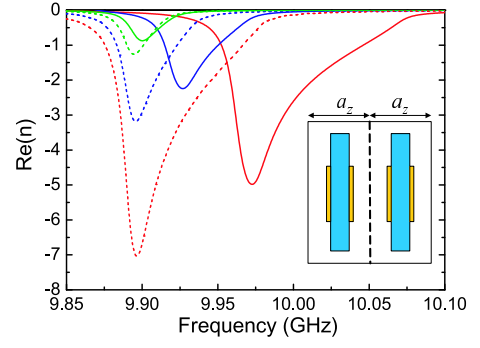


FIG. 9: Retrieved real part of refractive index,  $n$ , from simulated data using unit cell size in propagation direction  $a_z = 1$  mm (red),  $a_z = 2$  mm (blue) and  $a_z = 4$  mm (green). Both one layer (dashed) and two layers (solid) results are shown.

frequencies between one layer and two layer simulations are 77 MHz (red, with  $a_z = 1$  mm), 31 MHz (blue, with  $a_z = 2$  mm) and 6 MHz (green, with  $a_z = 4$  mm). It is shown that the resonance frequency,  $f_m$ , of two layers results decreases as  $a_z$  increases, while  $f_m$  of the one layer only shifts slightly, when the size of the unit cell increases. The frequency shift of two layers simulation is due to the coupling between the two neighboring layers of the fishnet. Notice that as the unit cell size  $a_z$  increases, the coupling between neighboring layers becomes weaker, and therefore the effective refractive index,  $\text{Re}(n)$ , of two layers approaches the one layer simulation results.

## CONCLUSIONS

We have systematically studied the size dependence of the retrieved parameters,  $\mu$ ,  $\epsilon$  and  $n$ , of the fishnet metamaterial structures as a function of the size of the unit cell. We found that the retrieval parameters have a **stronger** resonance behavior as the size of the unit cell decreases. We have also studied the convergence of the retrieved parameters as the number of the unit cells increases. We found that the convergence depends on the ratio of  $\lambda/a$ , where  $\lambda$  is the wavelength and  $a$  is the size of the unit cell. The larger  $\lambda/a$  is, the easier the convergence. The convergence of the fishnet structure is much slower than that observed in SRRs and/or wires systems. Finally, we gave an explanation of why the frequency width where  $n$  is negative is wider than the width where  $\mu$  is negative.

## ACKNOWLEDGMENTS

Work at Ames Laboratory was supported by Dept. of Energy (Basic Energy Sciences) under contract No. DE-AC02-07CH11358, by the AFOSR under MURI grant (FA9550-06-1-0337), by Dept. of Navy, office

of Naval Research (Award No. N0014-07-1-0359), EU FET projects Metamorphose and PHOREMOST, and by Greek Ministry of Education Pythagoras project.

- 
- [1] C. M. Soukoulis, M. Kafesaki, and E. N. Economou, *Advanced Materials* **18**, 1941 (2006).
- [2] C. M. Soukoulis, S. Linden, and M. Wegener, *Science* **315**, 47 (2007).
- [3] V. M. Shalaev, *Nature Photonics* **1**, 41 (2007).
- [4] S. Zhang, W. Fan, N. C. Panoiu, K. J. Malloy, R. M. Osgood, and S. R. J. Brueck, *Physical Review Letters* **95**, 137404 (pages 4) (2005), URL <http://link.aps.org/abstract/PRL/v95/e137404>.
- [5] G. Dolling, C. Enkrich, M. Wegener, C. M. Soukoulis, and S. Linden, *Optics Letters* **31**, 1800 (2006).
- [6] G. Dolling, C. Enkrich, M. Wegener, C. M. Soukoulis, and S. Linden, *Science* **312**, 892 (2006).
- [7] U. K. Chettiar, A. V. Kildishev, H. K. Yuan, W. Cai, S. Xiao, V. P. Drachev, and V. M. Shalaev, *Optics Letters* **32**, 1671 (2007), URL <http://www.opticsinfobase.org/abstract.cfm?URI=ol-32-12-1671>.
- [8] M. Kafesaki, I. Tsiapa, N. Katsarakis, T. Koschny, C. M. Soukoulis, and E. N. Economou, *Physical Review B (Condensed Matter and Materials Physics)* **75**, 235114 (pages 9) (2007), URL <http://link.aps.org/abstract/PRB/v75/e235114>.
- [9] D. R. Smith, S. Schultz, P. Markos, and C. M. Soukoulis, *Physical Review B (Condensed Matter and Materials Physics)* **65**, 195104 (pages 5) (2002), URL <http://link.aps.org/abstract/PRB/v65/e195104>.
- [10] T. Koschny, P. Markos, D. R. Smith, and C. M. Soukoulis, *Phys. Rev. E* **68** (2003).
- [11] T. Koschny, P. Markos, E. N. Economou, D. R. Smith, D. C. Vier, and C. M. Soukoulis, *Physical Review B (Condensed Matter and Materials Physics)* **71**, 245105 (pages 22) (2005), URL <http://link.aps.org/abstract/PRB/v71/e245105>.
- [12] D. R. Smith, D. C. Vier, T. Koschny, and C. M. Soukoulis, *Phys. Rev. E* **71**, 036617 (2005).
- [13] X. D. Chen, T. M. Grzegorzczak, B. I. Wu, J. Pacheco, and J. A. Kong, *Phys. Rev. E* **70**, 016608 (2004).
- [14] R. S. Penciu, M. Kafesaki, T. F. Gundogdu, E. N. Economou, and C. M. Soukoulis, *Photonics and Nanostructures: Fundamentals and Applications* **4**, 12 (2006).
- [15] J. F. Zhou, L. Zhang, G. Tuttle, T. Koschny, and C. M. Soukoulis, *Physical Review B (Condensed Matter and Materials Physics)* **73**, 041101 (pages 4) (2006), URL <http://link.aps.org/abstract/PRB/v73/e041101>.
- [16] M. W. McCall, A. Lakhtakia, and W. S. Weiglhofer, *European J. Phys.* **23**, 353 (2002).
- [17] R. A. Depine and A. Lakhtakia, *Microwave Opt. Technology Lett.* **41**, 315 (2004).
- [18] G. Dolling, M. Wegener, and S. Linden, *Optics Letters* **32**, 551 (2007), URL <http://www.opticsinfobase.org/abstract.cfm?URI=ol-32-5-551>.